Int. J. Heat Mass Transfer. Vol. 22, pp. 13–20
Pergamon Press Ltd. 1979. Printed in Great Britain

FREE CONVECTIVE HEAT TRANSFER TO FLUIDS IN THE NEAR-CRITICAL REGION FROM VERTICAL SURFACES WITH UNIFORM HEAT FLUX

T. R. SEETHARAM† and G. K. SHARMA‡
Department of Mechanical Engineering, Indian Institute of Technology, Bombay 400076, India

(*Received* 12 *April* 1978)

Abstract—Numerical predictions are made for laminar free convective heat transfer to fluids in the near-critical region from a vertical flat plate with uniform surface heat flux. The variation of all the thermophysical properties have been taken into consideration. The governing equations are integrated using the Patankar–Spalding implicit finite difference scheme. Computations are made for carbon dioxide at pressures of 75 ($P/P_{cr} = 1.015$), 80 ($P/P_{cr} = 1.083$) and 100 ($P/P_{cr} = 1.354$) bar and for water at pressures of 225 ($P/P_{cr} = 1.018$) and 245 ($P/P_{cr} = 1.108$) bar, for various values of wall-heat flux ranging from 1000 W/M^2 to 50000 W/M^2. Based on the results obtained, a correlation has been proposed to evaluate the local heat-transfer coefficient for a wide range of Rayleigh numbers ($Ra_\infty = 5 \times 10^6$–$5 \times 10^{10}$).

NOMENCLATURE

- x, coordinate measured in the direction of motion;
- y, coordinate measured normal to the direction of motion;
- u, velocity in the x direction;
- v, velocity in the y direction;
- g, acceleration due to gravity;
- P, pressure;
- T, temperature;
- i, enthalpy;
- h, heat-transfer coefficient;
- q, heat flux;
- ΔT, temperature difference between the wall and the ambient fluid, $(T_w - T_\infty)$;
- C_p, specific heat at constant pressure;
- $\bar{C}_p$, integrated mean value of $C_p(i_w - i_\infty)/\Delta T$;
- μ, dynamic viscosity;
- ρ, density;
- k, thermal conductivity;
- τ, shear stress;
- β, coefficient of thermal expansion;
- I, grid point counter;
- N, second grid point measured inward from the outer edge of the boundary layer;
- $NP2$, fictitious grid point at the outer edge of the boundary layer;
- $NP3$, grid point at the outer edge of the boundary layer.

Subscripts

- cr, properties corresponding to critical point;
- ∞, properties evaluated in bulk fluid;
- w, properties evaluated at the wall;
- c, refers to the edge of the Couette flow region;
- $*$, conditions corresponding to the peak value of C_p.

Non-dimensional parameters

- y_+, $= (\rho u/\mu)_c y$;
- u_+, $= u/u_c$;
- μ_+, $= \mu/\mu_c$;
- ρ_+, $= \dfrac{g\rho y_c}{(\rho u^2)_c}$;
- i_+, $= \dfrac{(i_w - i)(\rho u)_c}{q_w}$;
- τ_+, $= \tau/(\rho u^2)_c$;
- Pr, Prandtl number, $(\mu c_p/k)$;
- Ra, Rayleigh number, $(g\beta\Delta T x^3\rho^2/\mu^2)\cdot Pr$;
- Ra^*, Rayleigh number, $(g\beta q_w x^4\rho^2/k\mu^2)\cdot Pr$;
- Nu, Nusselt number, hx/k_∞.

†Research scholar.
‡Assistant professor.

INTRODUCTION

THE NECESSITY for studying the heat transfer to the fluids in the near-critical region has increased due to the recent use of near-critical fluids in various industrial applications. It is generally known that, near the critical region the process of heat transfer would become complicated due to the severe variation of the thermo-physical properties of the fluid, especially near the pseudo-critical point (which is defined as the point, where the specific heat at constant pressure becomes maximum). Typical variation of thermo-physical properties of carbon dioxide in the near-critical region at 75 bar is shown in Fig. 1. It has been established that conventional constant property correlations and theoretical models fail in predicting, accurately, the heat-transfer rates in the near-critical region.

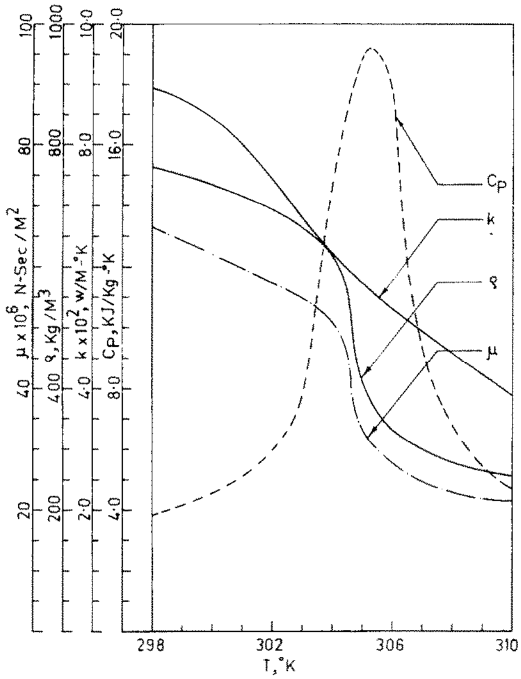

FIG. 1. Variation of properties of carbon dioxide at 75 bar.

A number of investigations, both theoretical and experimental, have been reported in the literature on free convective heat transfer to fluids in the near-critical region. All the analytical investigations [1–6], except the one by Ito *et al.* [7] have been carried out for the case of constant wall-temperature conditions. All the experimental investigations [8–12] have been confined to surfaces with practically uniform heat flux conditions. Ito *et al.* [7] have investigated the problem of free convective heat transfer to near-critical carbon dioxide from vertical plate with prescribed uniform heat flux by using an integral method. Accurate results cannot be obtained by using an integral method, because velocity and temperature profiles have to be assumed and no experimental data in the form of velocity and temperature profiles is available in the near-critical region.

The object of the present study is to use a more accurate method than the integral technique to investigate the problem of laminar free convective heat transfer to fluids in the near-critical region from a vertical plane surface with prescribed uniform heat flux. Two fluids, water and carbon dioxide are chosen for investigation. Numerical computations are made for water at pressures of 225 bar ($P/P_{cr} = 1.018$) and 245 bar ($P/P_{cr} = 1.108$) with $T_\infty = 370°C$ and for carbon dioxide at pressures of 75 bar ($P/P_{cr} = 1.015$), 80 bar ($P/P_{cr} = 1.083$) and 100 bar ($P/P_{cr} = 1.354$) with $T_\infty = 24.86°C$ for wide range of surface heat fluxes from 1000 W/m^2 to 50 000 W/m^2.

BASIC EQUATIONS

A semi infinite vertical flat plate with prescribed uniform heat flux is chosen as the physical model. Steady, two dimensional stable laminar boundary-layer flow conditions are assumed. For these conditions, equations for conservation of mass, momentum and energy may be written in the following form:

$$\frac{\partial}{\partial x}(\rho u) + \frac{\partial}{\partial y}(\rho v) = 0 \tag{1}$$

$$\rho u\left(\frac{\partial u}{\partial x}\right) + \rho v\left(\frac{\partial u}{\partial y}\right) = g(\rho_\infty - \rho) + \frac{\partial}{\partial y}\left(\mu \frac{\partial u}{\partial y}\right) \tag{2}$$

$$\rho u\left(\frac{\partial i}{\partial x}\right) + \rho v\left(\frac{\partial i}{\partial y}\right) = \frac{\partial}{\partial y}\left(\frac{k}{C_p}\frac{\partial i}{\partial y}\right) \tag{3}$$

with the boundary conditions of

$$u = v = 0; \quad -\left(\frac{k}{C_p}\right)\left(\frac{\partial i}{\partial y}\right) = q_w = \text{a constant at } y = 0$$

$$u = 0; \quad i = i_\infty \text{ at } y = \infty. \tag{4}$$

Since the velocities encountered in laminar free convective flows are very small, viscous dissipation is neglected. The cross stream independent variable, y is transferred to a dimensionless, normalised stream function, ω so that the finite difference grid, which is employed in the solution of the boundary-layer equations grows or contracts to fit the defined boundary layer. With the transformation the set of equations (1)–(3) can be written:

$$\frac{\partial u}{\partial x} + \left\{\frac{(\rho v)_I + [(\rho v)_E - (\rho v)_I]\omega}{(\phi_E - \phi_I)}\right\}\frac{\partial u}{\partial \omega} = g\frac{(\rho_\infty - \rho)}{\rho u} + \frac{\partial}{\partial \omega}\left[\frac{\rho u \mu}{(\phi_E - \phi_I)^2}\frac{\partial u}{\partial \omega}\right] \tag{5}$$

$$\frac{\partial i}{\partial x} + \left\{\frac{(\rho v)_I + [(\rho v)_E - (\rho v)_I]\omega}{(\phi_E - \phi_I)}\right\}\frac{\partial i}{\partial \omega} = \frac{\partial}{\partial \omega}\left[\frac{(\rho u \mu / Pr)}{(\phi_E - \phi_I)^2} \times \frac{\partial i}{\partial \omega}\right]. \tag{6}$$

The stream functions at the inner and outer edge of the boundary layer and the dimensionless stream function are then defined as follows:

$$\frac{d\phi_I}{dx} = -(\rho v)_I, \quad \frac{d\phi_E}{dx} = -(\rho v)_E, \quad \omega = \frac{\phi - \phi_I}{\phi_E - \phi_I}. \tag{7}$$

The finite difference forms of the equations (5) and (6) are obtained by integrating them over areas surrounding the grid points.

NUMERICAL SOLUTION

The resulting difference equations are solved using the Patankar–Spalding program [13]. The most significant feature of the Patankar–Spalding method is the one dimensional treatment of the region near the wall. Near a wall, the velocity, u is small and therefore, the convection in x direction is locally negligible. Thus near a wall, there exists a "Couette flow", i.e. a one dimensional flow in which the conditions are determined primarily by fluxes of momentum and energy across the boundary layer.

Therefore, for this region the flow can be described by ordinary differential equations which can be integrated directly to yield the values and slopes of the dependent variables at the edge of the Couette flow region. These values are used as boundary conditions for the finite difference solution, which is used from the edge of the Couette flow region to the outer edge of the boundary layer. This results in reducing the required number of cross stream grid points considerably.

The Patankar–Spalding program [13] is suitably modified to solve free convection problems. Another modification in the treatment of the Couette flow region is necessary to account for the severe variation of the thermophysical properties in the near-critical region. For the Couette flow region the simplified form of the momentum and energy equations are

$$\frac{d}{dy}\left(\mu\frac{du}{dy}\right)+g(\rho_\infty-\rho)=0 \tag{8}$$

$$\frac{d}{dy}\left(\frac{\mu}{Pr}\cdot\frac{di}{dy}\right)=0. \tag{9}$$

Equations (8) and (9) in terms of non dimensional parameters can be written as:

$$\frac{d}{dy_+}\left(\mu+\frac{du_+}{dy_+}\right)+\frac{1}{y_{+c}}[\rho_{+\infty}-\rho_+]=0 \tag{10}$$

$$\frac{\mu_+}{Pr}\frac{di_+}{dy_+}=1. \tag{11}$$

In order to integrate equations (10) and (11) the variations of ρ_+, μ_+ and Pr in the Couette flow region are required. In the Couette flow region, linear variation of ρ_+ and μ_+ with y_+ are assumed, as the temperature change across this region is small due to the small thickness of the region;

$$\rho_+=\rho_{+w}+\frac{(\rho_{+c}-\rho_{+w})y_+}{y_{+c}} \tag{12}$$

$$\mu_+=\mu_{+w}+\frac{(1-\mu_{+w})y_+}{y_{+c}}. \tag{13}$$

Using equations (12) and (13), equation (10) is integrated twice to give

$$\left(\mu_+\frac{du_+}{dy_+}\right)_w=\frac{(1-\mu_{+w})}{y_{+c}\ln(1/\mu_{+w})}+(\rho_{+\infty}-\rho_{+w})\left[\frac{1}{\ln(1/\mu_{+w})}-\frac{\mu_{+w}}{1-\mu_{+w}}\right]-\frac{(\rho_{+c}-\rho_{+w})}{4}\left[\frac{(1-3\mu_{+w})}{(1-\mu_{+w})\ln(1/\mu_{+w})}+2\left(\frac{\mu_{+w}}{1-\mu_{+w}}\right)^2\right]. \tag{14}$$

The variation of the Prandtl number in the near-critical region is similar to that of C_P and reaches a peak near the pseudo-critical temperature, T_*. Hence the integration of equation (11) is carried out for two separate cases:

Case (i): $T_C < T_W < T_*$ or $T_* < T_C < T_w$.

The Prandtl number variation is expressed as;

$$Pr=Pr_w+\frac{(Pr_c-Pr_w)i_+}{i_{+c}}. \tag{15}$$

Integration of equation (11) using (13) and (15) gives

$$i_{+c}=\frac{y_{+c}}{(1-\mu_{+w})}\ln(1/\mu_{+w})\ln\frac{(Pr_c-Pr_w)}{(Pr_c/Pr_w)}. \tag{16}$$

Case (ii): $T_C < T_* < T_w$.

For this case the Prandtl number variation can be expressed by two line segments

$$Pr=Pr_w+\frac{(Pr_*-Pr_w)i_+}{i_{+*}} \quad 0\leqslant i_+\leqslant i_{+*} \tag{17}$$

and

$$Pr=Pr_*+\frac{(Pr_c-Pr_*)(i_+-i_{+*})}{(i_{+c}-i_{+*})} \quad i_{+*}\leqslant i_+\leqslant i_{+c}. \tag{18}$$

Integration of equation (11) using (13), (17) and (18) gives

$$i_{+c}=i_{+*}-\left[\frac{i_{+*}}{Pr_*-Pr_w}\ln(Pr_*/Pr_w)+\frac{y_{+c}\ln(1/\mu_{+w})}{(1-\mu_{+w})}\right]\times\left[\frac{(Pr_c-Pr_*)}{\ln(Pr_c/Pr_*)}\right]. \tag{19}$$

The downstream profiles of velocity and enthalpy are determined using the set of finite difference equations simultaneously with equations (14) and (16) or (19). Properties of water in the near-critical region are taken from [15], while those for carbon dioxide are taken from [16]. A computer subroutine to interpolate, linearly the property values from these data is included in the program. For laminar flow, the ω-distribution, the entrainment rate and the initial profiles for velocity and temperature have to be specified. Near the critical region the Prandtl number is high ($Pr \gg 1$) and hence the region of significant temperature gradient will occupy a small portion of the velocity boundary layer. It is therefore necessary to provide an ω-distribution which will do justice to both velocity and thermal boundary layers. Near the wall and ω-spacings must be small; elsewhere they may be large. The distribution

$$\omega_I=\left(\frac{I-2}{NP2-2}\right)^2 \tag{20}$$

gave satisfactory results for all the cases studied. For a free outer boundary, the use of ω as the cross stream independent variable requires the specification of the entrainment rate into the flow for each downstream step. The entrainment rate is given by

$$(\rho v)_E=\frac{-2\mu_N+\mu_{NP3}}{Y_{NP3}+Y_N}. \tag{21}$$

The above formula is obtained by assuming a parabolic velocity profile and using the simplified form of the momentum equation at the outer edge of the boundary layer. The initial profiles required for this method are based on the polynomial profiles used for the integral solution of the constant property boundary layers under constant wall-heat flux conditions. 41 grid points are used and the solution is terminated at $Ra_{\infty} = 5 \times 10^{10}$.

RESULTS AND DISCUSSION

The velocity profiles for carbon dioxide at 75 bar for different values of the wall-heat flux are shown in Fig. 2. The maximum velocity in the boundary layer

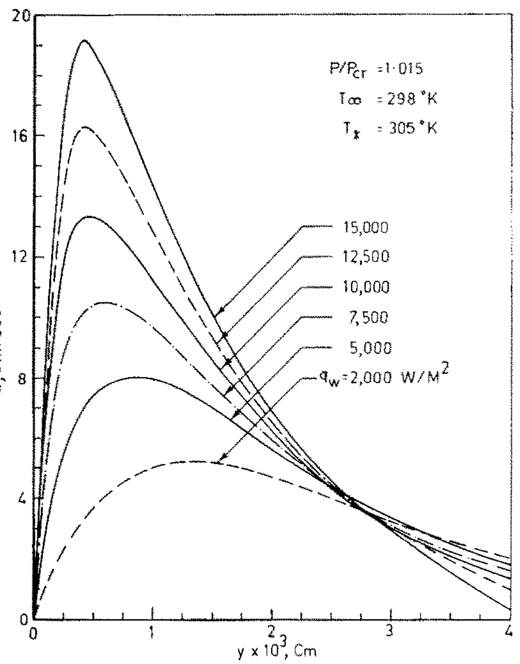

FIG. 2. Velocity profiles for carbon dioxide at 75 bar at $x = 0.03$ m.

increases with q_w and the location at which the maximum occurs shifts towards the wall as q_w increases. The temperature profiles, shown in Fig. 3 indicate that, whenever the value of q_w is such that T_* lies between the wall temperature and that of the ambient fluid, there is a distortion of the temperature profile. The distortion of the profile may be attributed to the nature of variation of C_P with temperature. For temperature less than T_*, C_P increases with temperature, while for temperatures greater than T_*, C_P decreases with the increase in temperature. The distortion occurs at a point where the slope dC_P/dT changes its sign. There is no distortion of the temperature profile for values of q_w which gives wall temperatures lower than T_*.

Figure 4 shows the variation of the heat-transfer coefficient with the wall-heat flux, q_w. The heat-transfer coefficient gradually increases with q_w until the wall temperature is several degrees (2–8°C) higher than T_*. Further increase in q_w results in decreasing the heat-transfer coefficient. In the near-critical region the heat-transfer coefficient depends not only on ΔT, but on the individual values of T_w and T_∞ as well. The severe variation of C_P in this region affects the temperature distribution in the

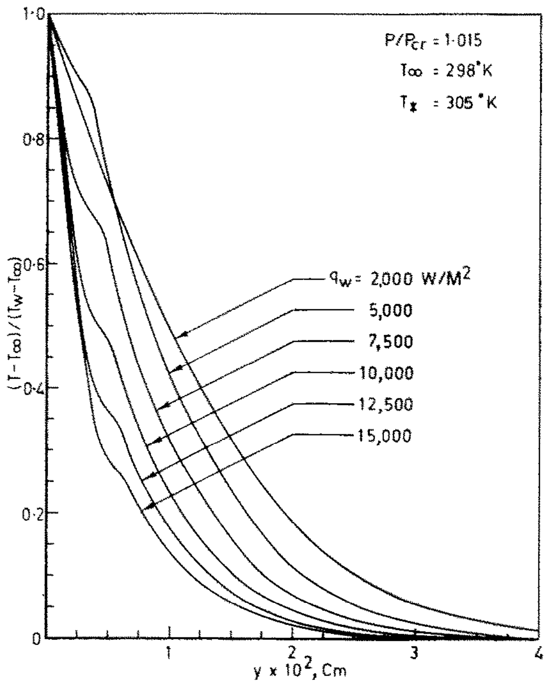

FIG. 3. Temperature profiles for carbon dioxide at 75 bar at $x = 0.03$ m.

boundary layer which in turn may decide the value of the heat-transfer coefficient. Figure 4 also indicates that for a specified value of q_w the heat-transfer coefficient increases as the pressure of the fluid approaches the critical value. The variation of the

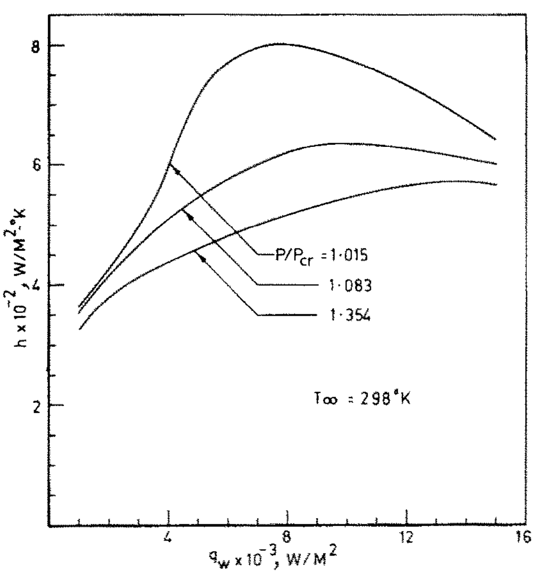

FIG. 4. Variation of heat-transfer coefficient with wall-heat flux at $x = 0.03$ m for different pressures.

temperature difference, ΔT with q_w presented in Fig. 5, indicates that ΔT increases with q_w. Also an inflexion point exists at a certain value of q_w for each pressure, which indicates a peak in the value of the heat-transfer coefficient. The wall temperature distribution for some typical values of q_w is presented in

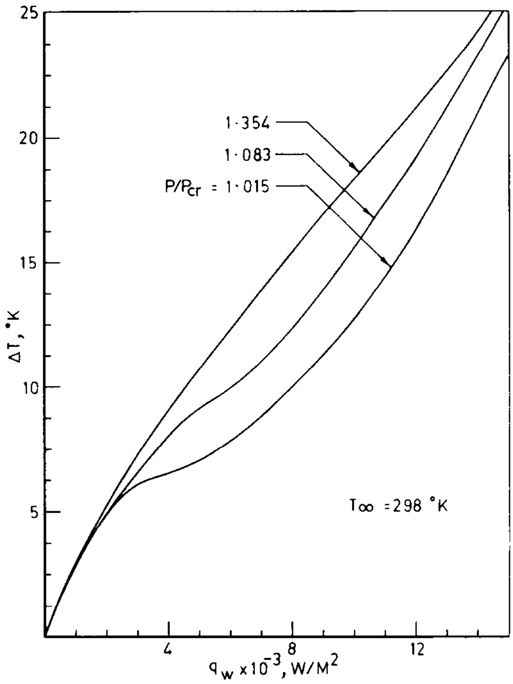

FIG. 5. Variation of temperature difference, ΔT with wall-heat flux at $x = 0.03$ m for different pressures.

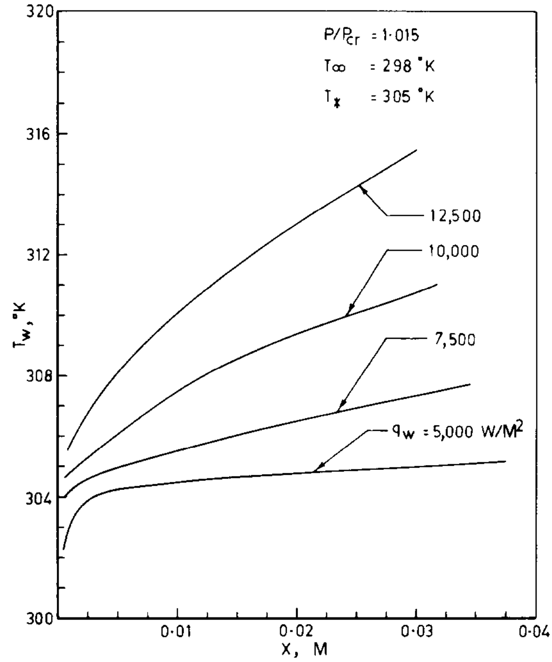

FIG. 6. Variation of wall-temperature with x for carbon dioxide at 75 bar.

Fig. 6. For values of q_w such that the wall temperature is in the neighbourhood of T_*, the increase of wall temperature with x is comparatively small. As the wall heat flux increases, the rate of increase of wall temperature becomes appreciable. The predicted wall temperatures are compared in Fig. 7 with the wall temperature distribution obtained by Sparrow and Gregg [14] for constant property case. In this figure, the constant property solution is indicated by the continuous curve and L represents the value of x at which $Ra_\infty^* = 10^{10}$. It can be observed that for low values of q_w such that the wall-temperature is lower than T_*, the predicted temperatures agree very well with those of Sparrow and Gregg. This can be expected because, when both T_w and T_∞ are much away from T_*, the variation of the physical properties is monotonic and gradual. However as q_w is increased so as to give wall temperatures in the neighbourhood of T_* the wall temperature distribution is quite different from that of Sparrow and Gregg.

Based on 352 data points for carbon dioxide, a correlation, to evaluate the local heat-transfer coefficient is obtained by the method of least squares. The correlation is

$$(Nu)_1 = 0.480(Ra_\infty)^{0.251}(\bar{C}_P/C_{P_\infty})^{0.491} \times (\rho_\infty/\rho_w)^{0.573}(\mu_\infty/\mu_w)^{-0.378}(k_\infty/k_w)^{-0.584}. \quad (22)$$

The above form was assumed to account for the variation of the physical properties in the near critical region. The maximum scatter of the data with respect to equation (22) is found to be $\pm 10\%$, the standard deviation being 7%. The scatter is more near the critical pressure and when the wall temperature is in the neighbourhood of T_*. For some typical conditions, Fig. 8 shows the comparison of equation (22) with the correlation suggested by Sharma and Protopopov [11]. Their correlation, based on experimental data gives higher values of heat-transfer coefficient (up to 20%) than those obtained using equation (22). This difference may be attributed to the fact that the deviation of the

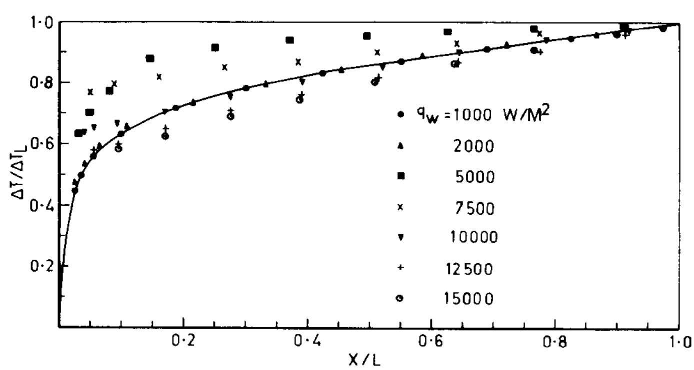

FIG. 7. Comparison of wall-temperature distribution for carbon dioxide at 75 bar with constant property solution.

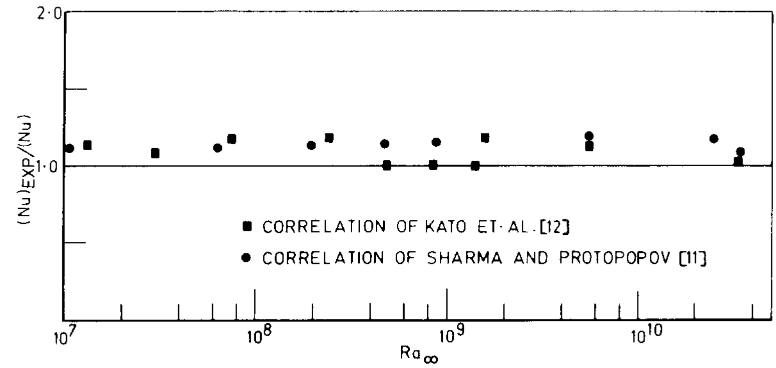

FIG. 8. Comparison of the present data with the available experimental data.

experimental data of Sharma and Protopopov from their correlation was found to be ±20%. Further they have obtained their experimental data for the case of free convective heat transfer from vertical tubes. In Fig. 8, the present correlation, equation (22) also is compared with the correlation suggested by Kato *et al.* [12]. Their correlation also predicts higher values of the heat-transfer coefficient than those obtained using equation (22). They have used integrated mean properties in their correlation and have found that their correlation gives higher values of heat-transfer coefficient (up to 25%) than their experimental data.

It is desirable to have a single correlation for different fluids and hence a correlation is obtained using 570 data points for water and carbon dioxide. The correlation is

$$(Nu)_2 = 0.475(Ra_\infty)^{0.250}(\bar{C}_P/C_{P_\infty})^{0.431} \times (\rho_\infty/\rho_w)^{0.089}(\mu_\infty/\mu_w)^{0.201}(k_\infty/k_w)^{-0.675}. \quad (23)$$

The maximum scatter of the data is found to be ±20%, the standard deviation being 13.55%. The two correlations, equation (22) and equation (23) are found to agree with each other within ±6%.

COMPARISION A

ΔT (°K)	x (M)	h_q/h_t
8·0	0·0045	1·092
8·0	0·0150	1·113
12·0	0·0100	1·115
12·0	0·0244	1·123
14·0	0·0075	1·098
14·0	0·0160	1·116
16·0	0·0110	1·104
16·0	0·0235	1·115
18·0	0·0155	1·113
18·0	0·0325	1·117

COMPARISION B

q_w (W/M²)	x (M)	h_q/h_t
7500	0·0100	1·065
7500	0·0478	1·135
10,000	0·0154	1·135
10,000	0·0266	1·140
10,000	0·0368	1·175
12,500	0·0104	1·150
12,500	0·0150	1·165
12,500	0·0210	1·170
12,500	0·0272	1·180
15,000	0·0102	1·160
15,000	0·0132	1·175

FIG. 9. Comparison between the values of heat-transfer coefficient for uniform wall-temperature and uniform wall-heat flux conditions.

In Fig. 9 the present solution for constant wall-heat flux conditions are compared with the authors' solution for constant wall temperature conditions [17]. Comparison is made for carbon dioxide at 75 bar. In this table h_q is the local heat-transfer coefficient for the present uniform heat flux condition and h_t, the local heat-transfer coefficient of the constant wall temperature solution [17]. In comparison *A* the plate surface temperatures in both the solutions are equal for the same elevation *x*, and in comparison *B* the surface heat fluxes are equal for the same elevation *x*. In comparison *A* the ratio, h_q/h_t is in the range from 1.09 to 1.12, whereas in comparison *B* the ratio is in the range from 1.07 to 1.18. Further in comparison *A*, the ratio is very nearly independent of *x* and *T*, whereas in comparison *B*, the ratio seems to depend on the values of both *x* and q_w.

CONCLUSIONS

Laminar free convection problems for fluids in the near-critical region under constant wall-heat flux conditions can be solved using the Patankar–Spalding method with suitable modifications of the wall functions to account for the severe variation of the physical properties in the near-critical region. The solutions obtained have indicated that, the wall-temperature distribution for near-critical fluids is quite different from that for fluids under conditions away from the critical region. Comparison of the solution for constant wall-heat flux conditions with that for constant wall-temperature conditions has shown that the heat-transfer coefficients for constant wall-heat flux conditions are 10–20% higher than those for constant wall-temperature conditions. Whenever the pseudo-critical temperature lies between the wall temperature and the ambient fluid temperature the temperature distribution in the boundary layer is distorted in the region, where the temperature corresponds to the pseudo-critical temperature. The correlation proposed to evaluate the local heat-transfer coefficients gives values which are within 20% from the available experimental data.

REFERENCES

1. C. A. Fritsch and R. J. Grosh, Free convective heat transfer to a supercritical fluid, in *Proceedings of the Heat Transfer Conference*, 1961, Part 2, Paper No. 121 (1961).
2. J. D. Parker and T. E. Mullin, Natural convection in the supercritical region, Symposium on Heat Transfer Fluid Dynamics of Near-Critical Fluids, *Proc. Instn Mech. Engrs* **182**(31), 1-5 (1968).
3. E. S. Nowak and A. K. Konanur, An analytical investigation of free convective heat transfer to supercritical water, *J. Heat Transfer* **92**(3), 345 (1970).
4. H. Kato, N. Nishiwaki and M. Hirata, Studies on the heat transfer of fluids at a supercritical pressure, *Bull. J.S.M.E.* **11**, 654–663 (1968).
5. S. Hasegawa and K. Yoshioka, An analysis for free convective heat transfer to supercritical fluids, in *Proceedings of the 3rd International Heat Transfer Conference*, Paper No. 63. A.I.Ch.E., New York (1966).
6. K. Nishikawa and T. Ito, An analysis of free convective heat transfer from an isothermal vertical plate to supercritical fluids, *Int. J. Heat Mass Transfer* **12**(11), 1449 (1969).
7. T. Ito, H. Yamashita and K. Nishikawa, Investigation of variable property problem concerning natural convection from vertical plate with prescribed uniform heat flux, in *Proceedings of the 5th International Heat Transfer Conference, Tokyo*, Paper No. NC 2.3. JSME-SCEJ, Tokyo (1974).
8. K. K. Knapp and R. H. Sabersky, Free convection heat transfer to carbon dioxide near the critical point, *Int. J. Heat Mass Transfer* **9**, 41 (1966).
9. H. A. Simon and E. R. G. Eckert, Laminar free convection in carbon dioxide near its critical point, *Int. J. Heat Mass Transfer* **6**, 681 (1963).
10. C. A. Fritsch and R. J. Grosh, Free convective heat transfer to supercritical water with experiments, *J. Heat Transfer* **85**, 289 (1963).
11. G. K. Sharma and V. S. Protopopov, Experimental investigation of natural convection heat transfer from a vertical surface to carbon dioxide at supercritical pressure, in *3rd National Heat Mass Transfer Conference*, IIT, Bombay, India, Paper No. HMT-35. 75 (1975).
12. H. Kato, N. Nishiwaki and M. Hirata, Studies on the heat transfer of fluids at a supercritical pressure, *Bull. J.S.M.E.* **11**, 658 (1968).
13. D. B. Spalding and S. V. Patankar, *Heat and Mass Transfer in Boundary Layers*. Inter Text, London (1970).
14. E. M. Sparrow and J. L. Gregg, Laminar free convection from a vertical plate with uniform surface heat flux, Paper No. 55-SA-4, ASME (1955).
15. S. L. Rivikin, *Thermophysical Properties for Water in the Critical Region* (in Russian). Izdatelstvo Standartov, Moscow (1970).
16. M. P. Vukalovich and V. V. Altunin, *Thermophysical Properties of Carbon Dioxide*. Moscow (1965).
17. T. R. Seetharam and G. K. Sharma, Numerical predictions of free convective heat transfer from vertical surfaces to fluids in the near critical region, in *4th National Heat and Mass Transfer Conference*, Rourkee, India, Paper No. 4 HMT-33 (1977).

CONVECTION THERMIQUE NATURELLE DE FLUIDES, PROCHES DE L'ETAT CRITIQUE, AU CONTACT DE SURFACES VERTICALES AVEC FLUX THERMIQUE UNIFORME

Résumé—Des calculs numériques sont développés pour la convection laminaire, naturelle de fluides proches de l'état critique et une surface plane verticale chauffée à flux uniforme. On prend en compte la variation de toutes les propriétés thermophysiques. Les équations sont intégrées en utilisant la méthode implicite aux différences finies de Patankar et Spalding. Des calculs sont effectués pour le gaz carbonique à 75 bar (P/P_{cr} = 1,015), 80 bar (P/P_{cr} = 1,083) et 100 bar (P/P_{cr} = 1,354) et pour l'eau à 225 bar (P/P_{cr} = 1,018) et 245 bar (P/P_{cr} = 1,108), avec des valeurs de flux pariétal variant de 1000 W/m^2 à 50 000 W/m^2. Basée sur les résultats obtenus, une formule est proposée pour évaluer le coefficient de transfert local, pour un large domaine de nombre de Rayleigh ($Ra_\infty = 5 \times 10^6$ à 5×10^{10}).

WÄRMEÜBERTRAGUNG DURCH FREIE KONVEKTION AN FLUIDE IM ÜBERKRITISCHEN GEBIET VON SENKRECHTEN FLÄCHEN MIT GLEICHFÖRMIGEM WÄRMESTROM

Zusammenfassung—Es werden numerische Berechnungen für die Wärmeübertragung durch laminare freie Konvektion an Fluide im nahkritischen Gebiet von senkrechten Flächen mit gleichbleibendem Wärmestrom durchgeführt. Es wurden die Veränderungen aller thermophysikalischen Eigenschaften berücksichtigt. Die maßgebenden Gleichungen wurden nach dem implizierten finiten Differenzen–Schema nach Patankar–Spalding integriert. Es wurden Berechnungen für Kohlendioxid bei Drücken von 75 bar (p/p_{kr} = 1,015); 80 bar (p/p_{kr} = 1,083) und 100 bar (p/p_{kr} = 1,354) und für Wasser bei Drücken von 225 bar (p/p_{kr} = 1,018) und 245 bar (p/p_{kr} = 1,108) durchgeführt, bei denen die Wand–Wärmestromdichten von 1000 bis 50 000 W/m^2 variiert wurden. Mit den erzielten Ergebnissen wurde die hier vorgeschlagene Beziehung entwickelt, mit der die örtlichen Wärmeübertragungskoeffizienten in einem weiten Bereich von Rayleigh–Zahlen ($Ra_\infty = 5 \times 10^6$ bis 5×10^{10}) berechnet werden können.

СВОБОДНОКОНВЕКТИВНЫЙ ПЕРЕНОС ТЕПЛА ОТ ВЕРТИКАЛЬНЫХ РАВНОМЕРНО НАГРЕВАЕМЫХ ПОВЕРХНОСТЕЙ К ЖИДКОСТЯМ В ОКОЛОКРИТИЧЕСКОЙ ОБЛАСТИ

Аннотация — Выполнены численные расчёты переноса тепла от вертикальной плоской равномерно нагреваемой пластины к жидкостям при ламинарной свободной конвекции в околокритической области с учётом изменения всех теплофизических характеристик. Исходные уравнения интегрировались с помощью неявной конечно-разностной схемы Патанкара-Сполдинга. Расчёты выполнены для двуокиси углерода при давлениях 75 ($P/P_{cr} = 1{,}015$), 80 ($P/P_{cr} = 1{,}083$) и 100 ($P/P_{cr} = 1{,}354$) бар и для воды при давлениях 225 ($P/P_{cr} = 1{,}018$) и 245 ($P/P_{cr} = 1{,}108$) бар при различных значениях плотности теплового потока на стенке в диапазоне от 1000 вт/м^2 до 50 000 вт/м^2. На основании полученных результатов предложено обобщенное соотношение для локального коэффициента теплообмена в широком диапазоне значений числа Релея ($Ra_\infty = 5 \times 10^6$ до 5×10^{10}).